2013 IEEE International Conference on Computer Vision Workshops

Separating Specular and Diffuse Reflection Components in the HSI Color Space

Jianwei Yang[1], Lixing Liu[2], Stan Z. Li[1*]
[1] CBSR & NLPR, Institute of Automation, Chinese Academy of Sciences, China
[2] Viterbi School of Engineering, University of Southern California, USA
[1]{jwyang, szli}@cbsr.ia.ac.cn; [2]lixingli@usc.edu

Abstract

In this paper, we propose to separate diffuse and specular reflection components for color images in the HSI color space. Under white illumination, pixels with the same diffuse chromaticity have the same hue. Meanwhile, specular pixels have lower saturations than the diffuse ones. Based on these properties, separating reflection components can be achieved by adjusting saturations of specular pixels to the values of diffuse-only pixels with the same diffuse chromaticity. We employ a region-growing algorithm to locate adjacent pixels with similar diffuse chromaticities. Then, the separation of reflection components is achieved by finding the optimal saturation in each connected region. The experimental results demonstrate that the proposed method is more effective to separate reflection components than the state-of-the-art methods.

1. Introduction

Specular reflections on surfaces often give rise to adjacent discontinuities in images. These discontinuities are usually omitted in computer vision tasks, which is not rational if the specular regions contain important information. Therefore, separating the diffuse and specular reflection components in color images plays an important role to improve high-level image understanding algorithms by recovering the hidden information. Meanwhile, explicitly obtaining the specular components also facilitates many algorithms which are directly based on specular components, such as shape from specular reflection [7].

Recently, many reflection components separation methods have been proposed for a single color image. Klinker et al. [5] introduced a T-shaped space, where one limb of the T-shaped distribution represents purely diffuse points while the other one corresponds to the specular components. In this space, the diffuse component is estimated via projecting the highlight limb to the diffuse one. However, the algorithm has a high computational complexity because of pixel-level image segmentation and T-shaped distribution analysis for each segment. Moreover, it may lose effectiveness when the T-shaped distribution is sparse. Alternatively, Bajscy et al. [1] proposed a specified three-dimensional space called S space. The S space is a HSI-type color space. However, to construct S_0 axis of S space, spectro-photometer is necessary to measure the scene radiance, which is not practical in many cases. Different from the previous works, Mallick et al. proposed a data-driven color space called SUV space in [9]. In this space, reflection components are transfered into S channel and UV channels, then the highlights are removed by iteratively eroding the specular channel using a family of non-linear partial differential equations (PDEs) [8]. Actually, when the illumination is known, all the procedures in SUV space can be transformed into RGB space. In this case, it is similar to T-Shaped space. Meanwhile, the guidance information for erosion introduces ambiguities among colors, and thus has bad effect on its separation results.

Different from the above three-dimensional spaces, the two-dimensional Maximum Chromaticity-Intensity space was proposed by Tan et al. [14]. In the space, the diffuse component is obtained by locally iterative process using the specular-free (SF) image as guidance, which can be finished without explicit image segmentation. Unfortunately, this method suffers from a high computational complexity and color distortions, especially at edge areas. To reduce computational complexity, Yang et al. [16] exploited a fast bilateral filtering technique. This method estimates the maximum diffuse chromaticity by directly applying a low-pass filter to the maximum fraction of the color components of the original image. However, the guidance image render ambiguities to the bilateral filter. Despite reducing the time cost significantly, this method results in color distortions at edge regions, as well as regions with uniform colors. In contrast, Yoon et al. [17] proposed an iterative framework based on the comparison of local ratios. In their method, a specular-free two band image was introduced. Local ratios between two pixels were computed in the input image

*Corresponding author.

978-0-7695-5161-6/13 $31.00 © 2013 IEEE
DOI 10.1109/ICCVW.2013.122

and specular-free two band image, respectively. Afterward, two reflection components were separated by making ratios between two pixels in input image and specular-free two band image equal to each other. Alternatively, Shen et al. [12, 11] used a modified specular-free (MSF) image. In their method, the specular component was estimated by using a Least Square Estimation (LSE) technique so that the transition regions between diffuse and specular pixels are smooth. However, this kind methods cause bad result due to ambiguity of MSF image in multi-colored specular regions. More recently, we proposed a novel 2-D space, namely Ch-CV space in [15]. Based on the Ch-CV space, a region-growing algorithm was implemented to separate reflection components. As we analyzed in [15], the HSI color space has similar properties to the Ch-CV space, which implies that HSI color space can also be used for the same task.

The aforementioned works were devoted to explore alternative spaces which can describe the specular and diffuse reflection components in a separable way. However, as a commonly used color space, the HSI color space itself is overlooked by the researchers. In this paper, we directly exploit the HSI color space to separate reflection components for a single color image. In our method, hue and saturation components are employed to construct a two-dimensional space, called H-S space. In the H-S space, there are two properties: 1) pixels with the same diffuse chromaticity have the same hue value, and thus assemble to be a line segment in the H-S space; 2) diffuse and specular pixels with the same diffuse chromaticity locate at different side of a line segment. Specifically, diffuse pixels have larger saturation than specular ones. Based on these properties, we implement region-growing algorithm used by our previous work [15] to locate connected regions with similar hues, and then estimate the reflection components for each pixel in each connected region.

2. Surface Reflection Model

2.1. Formulation

According to the dichromatic reflection model [10], the surface reflection can be described as the combination of specular reflection component and diffuse reflection component. Considering the spectral projection of camera sensors, the color intensities of pixels in an image are computed by the integration over the light spectrum:

$$I_c(x) = \omega_d(x) \int \tau_c(\lambda) S_d(\lambda, x) E(\lambda) d\lambda + \omega_s(x) \int \tau_c(\lambda) S_s(\lambda, x) E(\lambda) d\lambda \quad (1)$$

where $\omega_d(x)$ and $\omega_s(x)$ are the geometric scale factors of diffuse reflection and specular reflection, respectively, which merely depend on the geometry of a surface point; $\tau_c(\lambda)$ is the transmittance function of the camera sensor, and the subscript $c \in \{r, g, b\}$, represent red, green and blue channels; $E(\lambda)$ is the spectral power distribution of illumination light; $S_d(\lambda, x)$ and $S_s(\lambda, x)$ are the spectral distribution function of diffuse reflection and specular reflection, respectively.

Based on the assumption of neutral-interface-reflection (NIR) model [6], the color of specular reflection component is identical to illumination color. Therefore, $S_s(\lambda, x)$ is irrelevant to the color of surface point, which can be written as a constant, and absorbed into $\omega_s(x)$. Afterward, we define the diffuse chromaticity $\mathbf{\Lambda} = \{\Lambda_r, \Lambda_g, \Lambda_b\}$ and specular chromaticity $\mathbf{\Gamma} = \{\Gamma_r, \Gamma_g, \Gamma_b\}$ as

$$\Lambda_c(x) = \frac{\int \tau_c(\lambda) S_d(\lambda, x) E(\lambda) d\lambda}{\sum_c \int \tau_c(\lambda) S_d(\lambda, x) E(\lambda) d\lambda} \quad (2)$$

$$\Gamma_c = \frac{\int \tau_c(\lambda) E(\lambda) d\lambda}{\sum_c \int \tau_c(\lambda) E(\lambda) d\lambda} \quad (3)$$

Then, the color intensity of a pixel in channel $c \in \{r, g, b\}$ becomes

$$I_c(x) = m_d(x) \Lambda_c(x) + m_s(x) \Gamma_c \quad (4)$$

where

$$m_d(x) = \omega_d(x) (\sum_c \int \tau_c(\lambda) S_d(\lambda, x) E(\lambda) d\lambda) \quad (5)$$

$$m_s(x) = \omega_s(x) (\sum_c \int \tau_c(\lambda) E(\lambda) d\lambda) \quad (6)$$

Obviously, the sums of both the diffuse chromaticity vector $\mathbf{\Lambda}$ and the specular chromaticity vector $\mathbf{\Gamma}$ are equal to 1, i.e., $\sum_c \Lambda_c = \sum_c \Gamma_c = 1$. As a result, the sum of color intensities for a pixel $\sum_c I_c(x) = m_d(x) + m_s(x)$.

2.2. Illumination Chromaticity Normalization

In the real world, most illumination colors are not pure white, and the transmittance functions of camera sensors are different as well. Before separating the reflection components, we utilize the normalization approach introduced in [13] to obtain a whitened color image. Assuming that the estimated illumination chromaticity $\mathbf{\Gamma}^e = \{\Gamma_r^e, \Gamma_g^e, \Gamma_b^e\}$ is exactly equal to the real illumination chromaticity, we can derive the whitened image by dividing the estimated illumination chromaticity in both sides of Eq. (4):

$$\frac{I_c}{\Gamma_c^e} = m_d \frac{\Lambda_c}{\Gamma_c^e} + m_s \quad (7)$$

Then, we define $\Lambda_c' = \frac{\Lambda_c}{\Gamma_c^e} / \sum_c \frac{\Lambda_c}{\Gamma_c^e}$, thus,

$$I_c' = \frac{I_c}{\Gamma_c^e} = m_d' \Lambda_c' + \frac{m_s'}{3} \quad (8)$$

where $m_d' = m_d \sum_c \frac{\Lambda_c}{\Gamma_c^e}$ and $m_s' = 3 m_s$. Obviously, the sum of $\mathbf{\Lambda}'$ is still equal to 1, and the same to $\mathbf{\Gamma}'$.

3. Reflection Representation in H-S Space

In this section, we first elaborate the properties held by the H-S color space. Then, by comparing the H-S space with other color spaces specified for separating reflection components, we speculate that the H-S space is more suitable for the task because interference among different colors is reduced.

3.1. Analysis on H-S Space

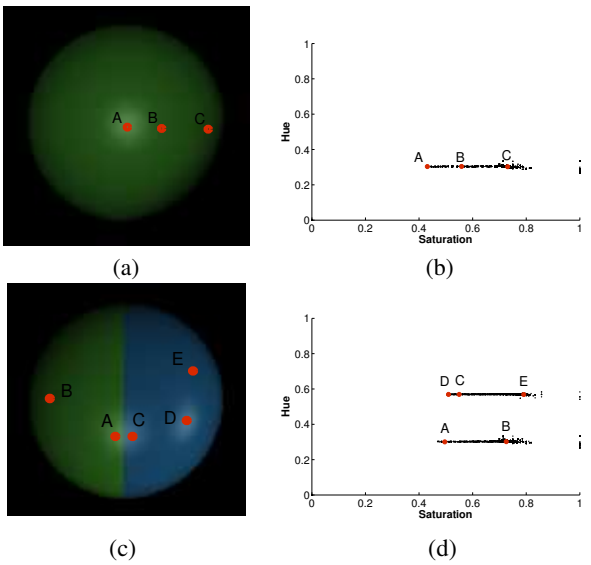

(a) (b) (c) (d)

Figure 1. (a) and (c) are synthetic images *green ball* and *blue-green ball*, respectively. (b) and (d) are their corresponding projections into H-S space.

In this part, we quantitatively analyze the properties of H-S space. According to [2], hue is formulated as:

$$H = cos^{-1}\left(\frac{\frac{1}{2}((I'_r - I'_g) + (I'_r - I'_b))}{((I'_r - I'_g)^2 + (I'_r - I'_b)(I'_g - I'_b))^{\frac{1}{2}}}\right) \quad (9)$$

Note that the hue is $2\pi - H$ when $I'_g < I'_b$. Based on Eq. (8), Eq. (9) is transformed to be:

$$H = cos^{-1}\left(\frac{3\sqrt{2}}{2}\frac{\Lambda'_r - \frac{1}{3}}{\sqrt{3\sum_c \Lambda'^2_c - 1}}\right) \quad (10)$$

Eq. (10) indicates that hue is merely determined by diffuse chromaticity $\mathbf{\Lambda'}$. In other words, pixels with the same diffuse chromaticity have identical hue. For illustration, we project two synthesized images into the H-S space shown in Fig. 1. As we can see, the single-colored *green ball* is projected to be a horizontal line, while the pixels in bi-colored image *blue-green ball* assemble to be two lines.

In the HSI color space, the saturation is computed by:

$$S = 1 - (\frac{3}{I'_r + I'_g + I'_b}) \min_c I'_c \quad (11)$$

Substituting Eq. (8) into the above equation, we have:

$$S = \frac{m'_d}{m'_d + m'_s}(1 - 3\min_c \Lambda'_c) \quad (12)$$

According to Eq. (12), given a group of pixels with consistent diffuse chromaticity $\mathbf{\Lambda'}$, the saturation is maximized for the diffuse-only surface points, i.e., $m'_s = 0$, and its value is exactly equal to $(1 - 3\min_c \Lambda'_c)$. As for the specular-only or monochromatic pixels, their saturations are identical to zero. With the increase of specular component, the saturation decreases gradually. The labeled points in Fig. 1 show the trend intuitively.

Based on the above analysis, we demonstrate that hue is merely relative to the diffuse component, and saturation is a measure of the combination level of diffuse and specular components.

3.2. Comparisons on Spaces

We compare H-S space with many color spaces specified for separating reflection components, including T-shaped space, S space, Maximum Chromaticity-Intensity space, SUV space and Ch-CV space.

- **T-shaped Space** [5]: It is totally embedded in the RGB color space. Based on the dichromatic reflection model, the colors of all reflections from one object form a planar cluster in the RGB color space, which is determined by the object and highlight colors and by the object shape and illumination. In this space, objects with different hues assemble in different planar clusters, and all these planes intersect at the direction of highlight color in RGB space..
- **S Space** [1]: S space is a 3-D color space formed with three orthogonal basis functions. To construct such space, it requires to measure spectral responses of sensors and determine the basis function for three axes, which, however, are not necessary for separating surface reflections. A simple HSI color space is enough to achieve it.
- **Maximum Chromaticity-Intensity Space** [14]: In this space, there is a non-linear relationship between maximum chromaticity and maximum intensity. According to the relationship between maximum chromaticity and saturation, this space can be feasibly replaced with the one spanned by saturation and intensity component in the HSI color space. Since the scanty of color information in this space, pixels with different diffuse chromaticity cannot be differentiate, it causes severe interference among different colors.

- **SUV Space** [9, 8]: It is a data-driven color space. Similar to the T-shaped space, it also rests on the RGB color space. Alternatively, it introduces a hue-like parameter θ and a saturate-like parameter ϕ. Afterward, a family of PDE filters are used to obtain diffuse contribution for each pixel. Actually, there is no need to trnasform the original RGB color space to SUV space. Once the illumination color is known, image can be first whitened and then the derivations of θ and ϕ are achieved in the RGB color space. Moreover, as a principle guidance for erosion, $\theta = \tan^{-1}(I_U/I_V)$ causes ambiguity when image has pixels with opposite sign of I_U and I_V, i.e., $\{I_U, I_V\}$ and $\{-I_U, -I_V\}$.
- **Ch-CV Space** [15]: We have shown in [15] that the Ch-CV space and H-S space both can separate pixels with different colors effectively. However, computing slopes in the Ch-CV space is of slightly higher computational complexity than deriving hues for a color image. Moreover, colors in the Ch-CV space distribute in a non-uniform manner. In this case, the region-growing algorithm performs relatively worse for images whose colors are concentrated around red, green or blue, and higher precision for yellow, cyan or purple.

Besides above explicitly defined color spaces, there are some other models based on color transformations. In [17], Yoon et al. introduced a specular-free two band image $\bar{I}$ and then computed two ratios r_d and r_{d+s} to guide the iteration process. However, the assumption that pixels in a local region have identical $\mathbf{\Lambda'}$ is often invalid for textured images, which causes interference among different colors. Similar ambiguity also occurs in the MSF image used in [12] and [11].

One of the critical problems for separating reflection components is how to construct a powerful space to identify the combination of specular components and diffuse components. Therefore, a color space proper for reflection separation needs to satisfy two principles: 1) specular pixels should be away from diffuse ones as far as possible; 2) pixels with different diffuse colors should be projected with the least interference. At this point, the the H-S space is similar to the S space, T-shaped space, Ch-CV space, and superior to the SUV space, Maximum Chromaticity-Intensity space and other specular-free image based models.

4. Reflection Components Separation

Given a whitened image, to separate reflection components means to decompose I'_c into $m'_d\Lambda'_c$ and $m'_s/3$ for each color channel $c \in \{r, g, b\}$. Based on Eq. (12) and $m'_d + m'_s = \sum_c I'_c$, m'_d can be written as:

$$m'_d = \frac{S \sum_c I'_c}{1 - 3\min_c \Lambda'_c} \tag{13}$$

Eq. (13) indicates that m'_d can be derived after obtaining the value of $(1 - 3\min_c \Lambda'_c)$ for each pixel. Afterward, m'_d, m'_s is obtained from $m'_s = \sum_c I'_c - m'_d$. Once we obtain m'_s for all pixels, their specular components are exactly $m'_s/3$, and their diffuse components are derived from $m'_d\Lambda'_c = I'_c - m'_s/3$. Therefore, the key step for separating reflection components is estimating $(1 - 3\min_c \Lambda'_c)$, which we call diffuse saturation considering it is the saturation of diffuse-only pixel.

4.1. Separation for Simple Color Image

For an image with simple colors, we can estimate the diffuse saturations for its pixels directly. According to Eq. (12), the diffuse saturation can be easily estimated by finding the most saturated pixels along a line segment in the H-S space, which is particularly applicable for simple color images. For example, pixels A, B, C in Fig. 1(a) have the same $\mathbf{\Lambda'}$, therefore we can estimate their diffuse saturations to be 0.79 approximately from Fig. 1(b). Similarly, there are two principle colors in Fig. 1(c), and their diffuse saturations are approximately 0.79 and 0.8, respectively. However, because of noises and distortions, pixels with the same hue assemble a line with a irregular tiny width. In this case, the diffuse saturation cannot be estimated accurately by finding the most saturated pixels along a line segment. We can assign all pixels in a hue interval with the same diffuse saturation.

4.2. Region-Growing Algorithm

For images with various colors and textures, there are still some challenges in the separation process, which are elaborated in the following cases:

- **Case A**: In a multi-colored image, there may exist pixels with the same hue but different $\mathbf{\Lambda'}$, which happens when pixels have identical diffuse hue yet different diffuse saturations. To solve this problem, we assume that pixels with different diffuse saturation are spatially separative. In other words, there is no connected region with uniform hue but a smooth saturation. Based on this assumption, the diffuse saturation can be derived by finding the most saturated pixels in a connected region with similar hues.
- **Case B**: The most saturated pixels in a connected region are usually not the exact diffuse-only ones. It is acceptable if specular components on those pixels are minor. However, it is occasionally the case that some pixels are all polluted by intense specularities. For these pixels, we estimate their specularities directly using neighboring context, rather than estimating their diffuse saturations. Concretely, we use the correctly estimated specular components in their neighbors to estimate their specularities.

To address the problem discussed in **Case A**, we use a 8-connected region-growing algorithm in [4] to obtain the connected image regions with similar hues in the H-S space. In this paper, the uniformity parameter is set to be a constant value 10 on condition that hue ranges in $[0, 360)$. As analyzed in **Case B**, pixels in some connected regions may all have intense specularities. We call this kind of regions as specular connected regions, and the others as specular-diffuse connected regions. Because specular connected regions are more likely to have small sizes, we regard regions with sizes less than a threshold T_a as specular connected regions, and the others as specular-diffuse connected regions. In our algorithm, $T_a = 20$. Note that we use the highlight detection method presented in [15] to determine the specular pixels in an image before conducting the region-growing algorithm.

For a specular-diffuse region G, the diffuse saturations for all pixels in it are estimated to be the largest saturation value $\in G$. The estimation procedure is briefly presented in **Algorithm** 1. In the algorithm, $Opt(R_i)$ means to get the optimal saturation S in the specular connected region R_i, which is generally equal to $\max_{x \in R_i} S(x)$. However, to avoid the effects of random noises and make the transition from diffuse to specular regions smooth, we alternatively set the optimal S to be $\arg_S \pi(S) = 0.1$, which means there are 10% pixels lying between the optimal S and $\max_{x \in R_i} S(x)$. After obtaining the diffuse saturations for all pixels in specular-diffuse connected regions, m'_d is then calculated for all pixels using Eq. (13).

Algorithm 1 Estimation of diffuse saturations for specular pixels in specular-diffuse connected regions.

Input variables: R_i = i^{th} specular-diffuse connected region; N = number of specular-diffuse connected regions.
Local variables: S_{opt} = the optimal S for specular-diffuse connected region;

1: **for** $i \leftarrow 1$ **to** N **do**
2: $\quad D_{opt} \leftarrow Opt(R_i)$
3: $\quad (1 - 3 \min_c \Lambda'_c(x)) \leftarrow S_{opt}\ \forall x \in R_i$
4: **end for**

As for the pixels in specular connected regions, we estimate their specular reflection components directly after obtaining specular components of pixels in all specular-diffuse connected regions. We determine their specular components by using a mean-filter with size of 5×5 from outside to inside. Once we obtain m'_s for all specular pixels, their specular components and their diffuse components are derived from $m'_s/3$ and $I'_c - m'_s/3$, respectively. Furthermore, the diffuse chromaticity $\mathbf{\Lambda'}$ can be obtained by dividing the diffuse component by m'_d.

5. Experiments

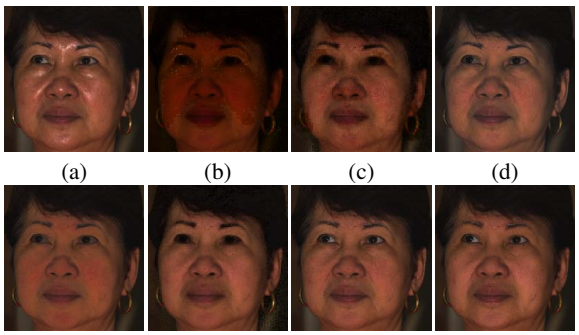

Figure 2. Diffuse reflection component recovered from *lady*. (a) is the input image. The others are diffuse components estimated based on (b) [14], (c) [17], (d) [12], (e) [11], (f) [16], (g) [15], and (h) the proposed method.

In our experiments, we compare the results of our method with six previous methods proposed by Tan et al. [14], Yoon et al. [17], Shen et al. [12, 11], Q.X. Yang et al. [16], and our own method [15]. For evaluation, we use 13 test images from previous works and two images with ground-truth from [3].

In Fig. 2, we first use a real-world image *lady* to evaluate the reflection component separation performance. As we can see, our methods have better performance in terms of color smoothness and distortion. [14], [17], and [11] have poor performance because they do not take into account color discontinuities. In contrast, Algorithms in [12] and [16] achieve slightly better performance since they cause less confusions among different colors. However, both the MSF image used in [12] and guidance image used in [16] introduce interference among colors with different hues. In comparison, the methods in [15] and our methods achieve comparable results and outperform the other methods.

Two real-world images with multicolored and textured surfaces are used to compare the performance. In Fig. 3, the first two rows shows the recovered diffuse components of a real-world image *fish*, and the bottom two rows shows the projections of the diffuse components in the region labeled with red boundary. As we can see, the method in [14] results in a severely over-saturated diffuse component. Because its neighbor-based iteration algorithm cannot distinguish pixels with different colors, severe color distortions occur at edges which further spread inside to all pixels. Similarly, in [17], the iteration algorithm assumes that neighbor pixels have identical diffuse chromaticity, and thus results in many color distortions at edges and inside color regions as well. [12] detects the highlight regions first, and then conducts a local LSE algorithm for pixels with similar values

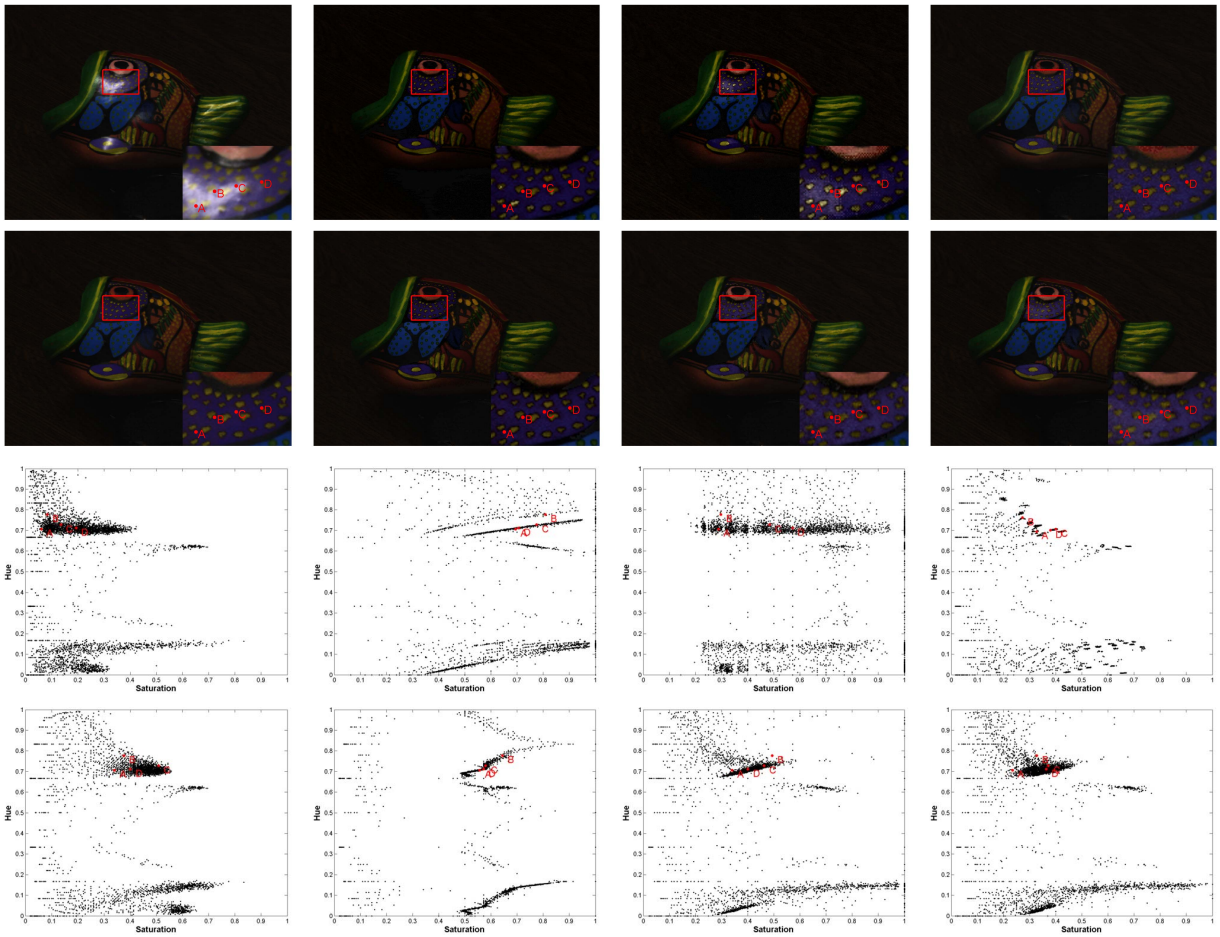

Figure 3. Diffuse components of image *fish* recovered by different methods. The display arrangement is same to that of Fig. 2. In the bottom two rows, we project the diffuse components inside the red rectangle into the H-S space. Four points are labeled for comparison.

in the MSF image. It has better performance than the previous two methods. However, it assigns all pixels which have similar MSF value with the same diffuse component, which makes the subjective effects bad. Alternatively, [11] implements the LSE algorithm for each specular region, rather than region with similar values in MSF image. This method is faster than [12], however, at the cost of separation performance. Though the method in [16] accelerates the separation process significantly, its result also has severe saturation distortions, because bilateral filtering is confused by the guidance image. In comparison, by introducing the reflectance separation model base on the HSI color, we obtain more accurate diffuse chromaticity for specular regions by ruling out interference among pixels with different hues. The specular pixels are successfully drawn back to the diffuse ones with less saturation distortions. A similar result is obtained by [15]. The comparison on another real world image *toys* presented in Fig. 4 also offers support to our claim.

To evaluate the methods quantitatively, we compute the peak signal-to-noise ratio (PSNR) between the recovered diffuse components and the ground-truth in non-zero regions for two test images: *apple* and *pear-mit*. As we can see, the proposed method achieves the highest PSNR, and the results from [12], [16] and [15] are competitive because all of them take the color differences into account. Among these three methods, the performance of [15] is most remarkable. However, because of the densely distributed colors in the Ch-CV space for the two test images, the precision of region-growing algorithm degrades.

In Fig. 7, we compare the logarithmic runtime of all methods. As we can see, since the proposed method needs no iterative process for each pixel, its computational complexity is lower than the methods in [14] and [17], higher than the methods in [11] and [16], and analogous to [12] and [15].

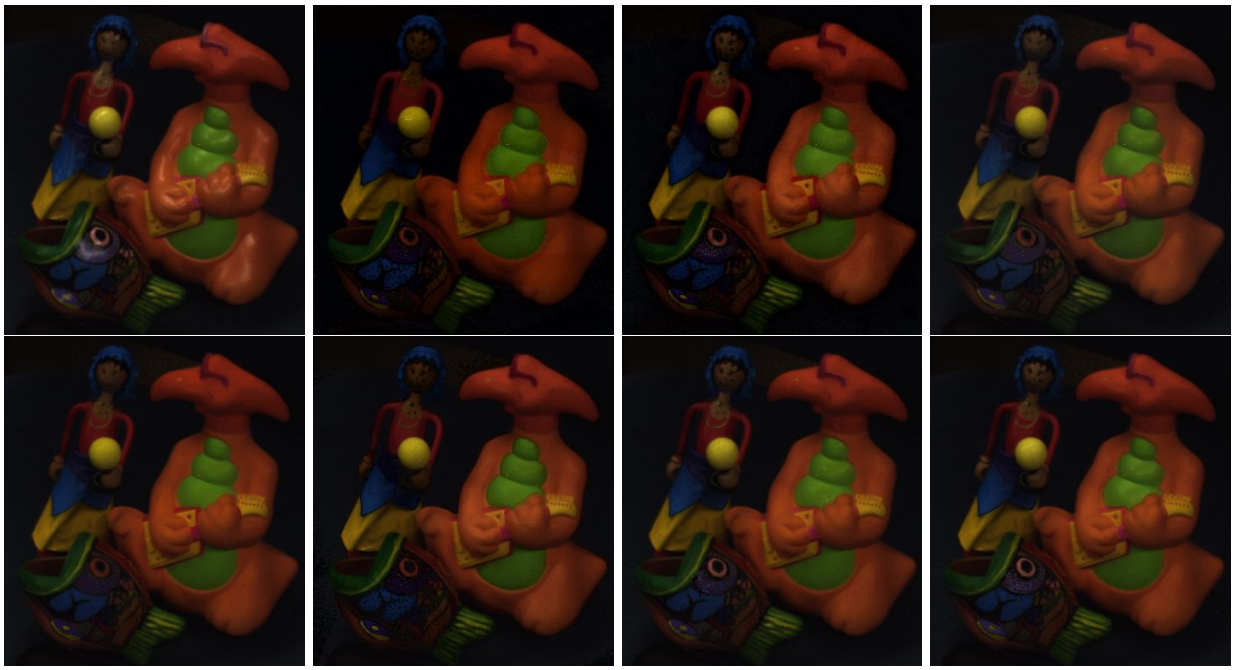

Figure 4. Diffuse components of image *toys*. The display arrangement is same to that of Fig. 2.

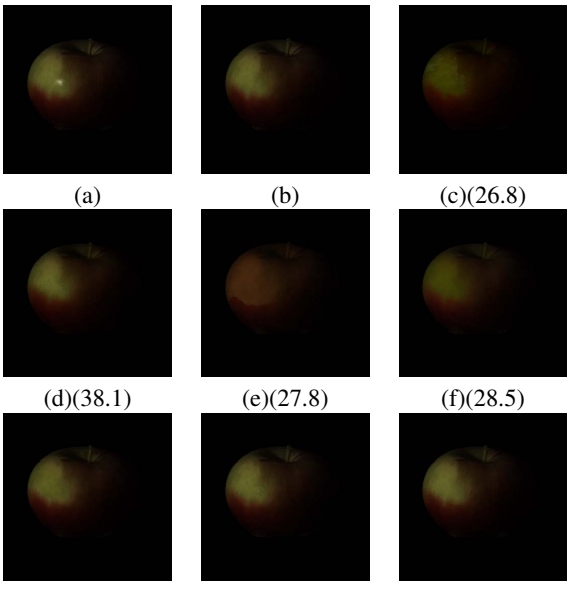

(a) (b) (c)(26.8)

(d)(38.1) (e)(27.8) (f)(28.5)

(g)(41.1) (h)(44.3) (i)(44.8)

Figure 5. Quantitative comparison on image *apple*. Form top left to bottom right, the images are: (a) input images, (b) ground truth, diffuse components from (c) [14], (d) [17], (e) [12], (f) [11], (g) [16], (h) [15], and (i) the proposed method. The corresponding PSNR (dB) values are reported below each image.

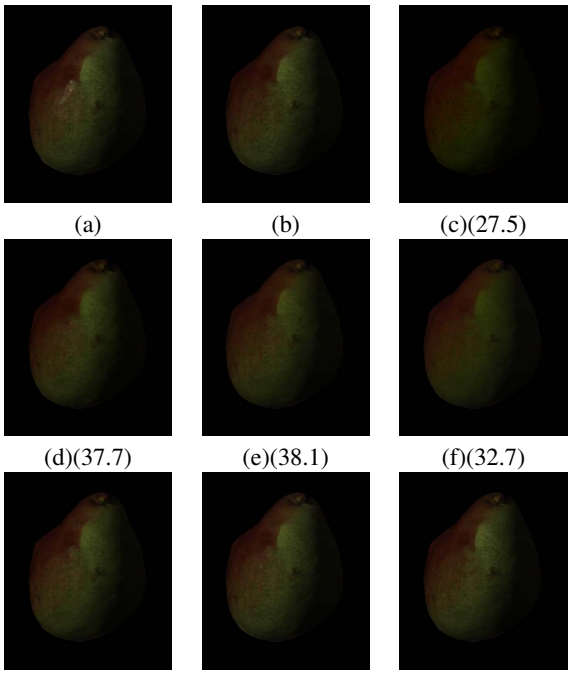

(a) (b) (c)(27.5)

(d)(37.7) (e)(38.1) (f)(32.7)

(g)(39.4) (h)(40.1) (i)(42.1)

Figure 6. Quantitative comparison on image *pear-mit*. The order is same to Fig. 5.

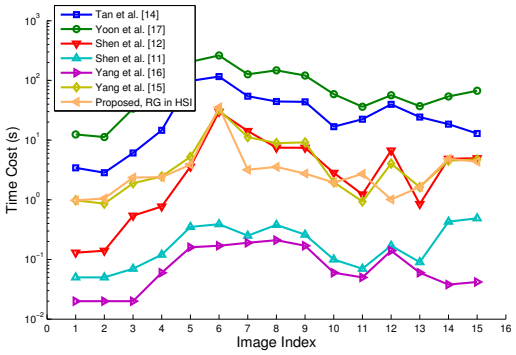

Figure 7. Logarithmic time costs. The index corresponds to images: *ball-green*, *ball-blue-green*, *synth*, *head*, *pear*, *fish*, *toys*, *bear*, *bear2*, *red-pear*, *red-pear2*, *train*, *lady*, *apple*, and *pear-mit*.

6. Conclusion

In this paper, we have proposed a novel reflection components separation model based on H-S color space. Compared with other color spaces specified to the separation task, in the H-S space, the interference among pixels with different colors is minimal. Separating reflection components in the H-S space is finding the most saturated pixels in a specular region with similar hues, which can be achieved based on region-growing algorithm. We conducted experiments on both synthesized and real-world images to compare the performance with previous works. The results proved the superiority of the H-S space, and the efficiency of proposed separation algorithm as well.

Acknowledgement. This work was supported by the Chinese National Natural Science Foundation Project #61070146, #61105023, #61103156, #61105037, #61203267, #61375037, National IoT R&D Project #2150510, National Science and Technology Support Program Project #2013BAK02B01, Chinese Academy of Sciences Project No. KGZD-EW-102-2, European Union FP7 Project #257289 (TABULA RASA), and AuthenMetric R&D Funds.

References

[1] R. Bajcsy, S. W. Lee, and A. Leonardis. Detection of diffuse and specular interface reflections and inter-reflections by color image segmentation. *International Journal of Computer Vision*, 17(3):241–272, 1996.

[2] R. C. Gonzalez and R. E. Woods. *Digital image processing*. Addison-Wesley, 1992.

[3] R. Grosse, M. K. Johnson, E. H. Adelson, and W. T. Freeman. Ground-truth dataset and baseline evaluations for intrinsic image algorithms. In *International Conference on Computer Vision*, pages 2335–2342, 2009.

[4] S. Hojjatoleslami and J. Kittler. Region growing: A new approach. *IEEE Transactions on Image Processing*, 7:1079–1084, 1995.

[5] G. Klinker, S. A. Shafer, and T. Kanade. The measurement of highlights in color images. *International Journal of Computer Vision*, 2(1):7–32, 1988.

[6] H.-C. Lee, E. J. Breneman, and C. P. Schulte. Modeling light reflection for computer color vision. *IEEE Trans. Pattern Anal. Mach. Intell.*, 12(4):402–409, 1990.

[7] J. Lellmann, J. Balzer, A. Rieder, and J. Beyerer. Shape from specular reflection and optical flow. *International Journal of Computer Vision*, 80(2):226–241, 2008.

[8] S. P. Mallick, T. Zickler, P. N. Belhumeur, and D. J. Kriegman. Specularity removal in images and videos: A pde approach. In *ECCV (1)*, pages 550–563, 2006.

[9] S. P. Mallick, T. Zickler, D. J. Kriegman, and P. N. Belhumeur. Beyond lambert: Reconstructing specular surfaces using color. In *CVPR (2)*, pages 619–626, 2005.

[10] S. Shafer. Using color to separate reflection components. *Color Research and Applications*, 10:210–218, 1985.

[11] H.-L. Shen and Q.-Y. Cai. Simple and efficient method for specularity removal in an image. *Applied Optics*, 48:2711–2719, 2009.

[12] H.-L. Shen, H.-G. Zhang, S.-J. Shao, and J. H. Xin. Chromaticity-based separation of reflection components in a single image. *Pattern Recognition*, 41(8):2461–2469, 2008.

[13] R. Tan, K. Nishino, and K. Ikeuchi. Color constancy through inverse intensity chromaticity space. *JOSA*, 21(3):321–334, 2004.

[14] R. T. Tan and K. Ikeuchi. Separating reflection components of textured surfaces using a single image. *IEEE Trans. Pattern Anal. Mach. Intell.*, 27(2):178–193, 2005.

[15] J. Yang, Z. Cai, L. Wen, Z. Lei, G. Guo, and S. Z. Li. A new projection space for separation of specular-diffuse reflection components in color images. In *ACCV (4)*, pages 418–429, 2012.

[16] Q. Yang, S. Wang, and N. Ahuja. Real-time specular highlight removal using bilateral filtering. In *ECCV (4)*, pages 87–100, 2010.

[17] K.-J. Yoon, Y. Choi, and I.-S. Kweon. Fast separation of reflection components using a specularity-invariant image representation. In *ICIP*, pages 973–976, 2006.